

Transworld Research Network
37/661 (2), Fort P.O., Trivandrum-695 023, Kerala, India



Recent Res. Devel. Biophysics, 3(2004): ISBN: 81-7895-130-4

Modeling the cellular basis of cardiac excitation-contraction coupling and energy metabolism

**My-Hanh T. Nguyen¹, Hena R. Ramay¹, Stephen J. Dudycha²
and M. Saleet Jafr¹**

¹Program in Bioinformatics and Computational Biology, School of Computational
Sciences, George Mason University, Manassas, VA 20110, USA; ²Diagnostic
Ultrasound Woodinville, WA 98072, USA

Introduction

The use of mathematical formalism to understand the complex mechanism that govern the beating of the heart has a long history starting with the system cardiac physiologists who described phenomenon such as the generation of force by mathematical relations such as Starling's Law. This tradition was continued by the electrophysiologists who by their training naturally thought about the electrical properties of the heart in a quantitative fashion and by others in the field. As a result, there has been a large amount of quantitative data gathered on the heart. Furthermore, mathematical and computational modeling of the heart has long been regarded as a useful exercise or tool in understanding the heart.

Two areas that have benefited from mathematical and computational models are cardiac excitation-contraction (EC) coupling and energy metabolism. Both these systems are complex and the formulation of computational models has enabled predictions to be made and hypotheses to be tested about the mechanisms that govern their behavior. This manuscript describes some recent advances in modeling cardiac EC coupling and energy metabolism and the contributions these efforts have advanced understanding of the heart function on a cellular level.

Cardiac excitation-contraction coupling

Calcium (Ca^{2+}) plays a highly crucial role in proper functioning of the heart [1]. A combination of diverse effects mediated by Ca^{2+} ions gives rise to contraction and relaxation of the chambers of the heart to pump blood. This process, called EC coupling begins with the electrical excitation of cardiac myocytes and ends with the activation of the myofilaments which cause the contraction of the myocytes [2].

Excitation of the cardiac myocytes is initiated when an action potential (AP), a membrane potential (E_m) waveform, depolarizes the plasma membrane (sarcolemma). AP is determined by a complex series of ionic currents through channels and transporters in the sarcolemma [3]. During diastole, the sarcolemma is selectively permeable to K^+ ions through the voltage gated K^+ channels which dictate the resting E_m in myocytes. The rising phase of the AP is initiated by the activation of voltage-gated Na^+ channels followed by opening of voltage-gated L-type Ca^{2+} channels (I_{Ca}). The upstroke of AP ends with the inactivation of Na^+ channels and relayed rectifier K^+ channels. The balance of K^+ efflux (I_K) and Ca^{2+} influx (I_{Ca}) produces the long plateau of depolarization. Finally, the inactivation of voltage-gated Ca^{2+} channels terminates the plateau and the dominant K^+ channels repolarizes the E_m . It is important to note here that substantial interspecies differences in mammalian cardiac AP exist and are primarily attributed to differences in I_K and I_{Ca} time courses [4].

Calcium influx during depolarization triggers Ca^{2+} release through Ca^{2+} -activated ryanodine receptors (RyR) present in the junctional SR and elevates intracellular Ca^{2+} concentration $[\text{Ca}^{2+}]_i$ in a restricted area called the dyadic cleft in a process called Ca^{2+} -induced Ca^{2+} release (CICR) [5]. Spontaneous Ca^{2+} release events in the dyadic cleft are called Ca^{2+} sparks [6]. A summation of these transient local events is thought to give rise to the whole Ca^{2+} transient and contraction [7, 8].

Calcium released from the sarcoplasmic reticulum results in myofilament crossbridge formation and subsequent contraction [9]. Some of the Ca^{2+} released binds with troponin C which activates the contractile machinery consisting of actin and myosin filaments. After contraction, the cell must relax. For

relaxation, Ca^{2+} is extruded from the cytoplasm by $\text{Na}^+/\text{Ca}^{2+}$ exchanger (NCX) and sarcolemmal Ca^{2+} -ATPase pumps and sequestered into SR by Sarcoplasmic/Endoplasmic Ca^{2+} -ATPase pumps (SERCA) with different contributions depending on the species.

Cardiac excitation-contraction models

There have been several successful attempts to model the cardiac ventricular action potential starting with the DiFrancesco-Nobel model for the mammalian ventricular myocyte [10] and continuing to more recent models such as the Luo-Rudy Phase II model for guinea pig [11, 12]. While these models very successfully captured the ventricular action potential, they used phenomenological descriptions of Ca^{2+} dynamics that captured some of the behavior, but failed to truly capture the mechanisms. This omission was due to the difficulty in capturing the high gain (positive feedback) present during Ca^{2+} -induced Ca^{2+} release while still maintaining stability of the model. High gain is the observation that Ca^{2+} release from the SR is significantly larger than the I_{Ca} trigger [5].

The Jaffr-Rice-Winslow (JRW) model [13] and improvements thereof [14, 15] incorporate a biophysical description of the mechanisms of Ca^{2+} dynamics into the Luo-Rudy Phase II model. Figure 1A schematically shows the model. The JRW model successfully describes Ca^{2+} dynamics by creating a new

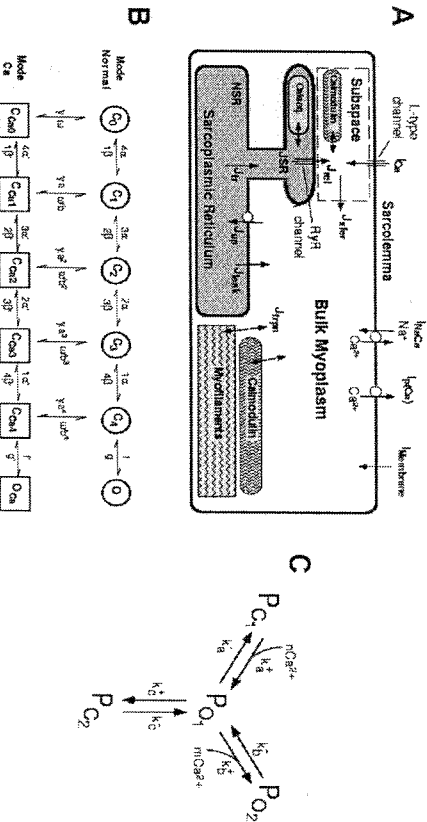


Figure 1. A. Schematic diagram for the model of the Jafri-Rice-Winslow guinea pig ventricular cell model. B. Markov state diagram for the L-type Ca^{2+} channel used in the JRW model. C. Markov state diagram of the Keizer-Levine model for the RyR channel that was used in the JRW model.

Markov state model formulation of the L-type Ca^{2+} channel and using the Markov state model for the RyRs created by Keizer and Levine [16] and describing their interaction in a restricted subspace (i.e. the dyadic space).

L-type Ca^{2+} channels are activated by membrane depolarization from -40 mV to $+10$ mV and contribute to the long plateau of the AP. L-type Ca^{2+} channels are known to inactivate through voltage- and Ca^{2+} -dependent mechanisms [17]. Calcium dependent inactivation has a much faster time course of development than voltage-dependent inactivation and plays a major role in inhibition of Ca^{2+} influx into the cell. The major determinant of the inactivation kinetics of Ca^{2+} current during depolarization is Ca^{2+} -dependent mechanisms [18]. The L-type Ca^{2+} channel model describes Ca^{2+} -dependent inactivation by mode switching as first suggested by Imredy and Yue [19] and included voltage dependent activation and inactivation. Figure 1B shows Markov state diagram for the JRW L-type Ca^{2+} channel model. The states C_0 through C_4 indicate closed states where 0 through 4 of the channel's 4 subunits are in the permissive state, respectively (similarly for states C_{a0} through C_{a4}). The O states indicate the open state. The top row is denoted "mode normal" and the bottom row is denoted "mode Ca^{2+} ". The transition from mode normal to mode Ca^{2+} is dependent. The rightward and leftward transitions are voltage-dependent transitions, indicating activation and deactivation of the channel. The transition from C_4 to O is fast and voltage-independent, while the transition from C_{a4} to O_{Ca} is slow and voltage-independent. The net result is that channel openings are infrequent in mode Ca^{2+} .

RyRs are the Ca^{2+} -sensitive Ca^{2+} release channels in the SR. Bilayer data shows that in response to a step increase in Ca^{2+} , the open probability of the channels rapidly increases and then declines to a level above the original baseline [20]. This phenomenon was termed adaptation. Keizer and Levine [16] proposed a minimal four state model for the RyR channel in which the channel was sensitive to bulk myoplasmic Ca^{2+} . The RyR model was based on the bilayer data showing open and dwell times as well as adaptation. (Figure 1C). In this model state P_{Cl} is closed state, P_{O1} and P_{O2} are the open states, and P_{C2} is the adapted state. However, in cardiac myocytes, experimental observation indicate confinement of these channels to a restricted space called the dyadic space or subspace in apposition to the L-type channels where $[\text{Ca}^{2+}]$ elevations were much greater than the average $[\text{Ca}]_i$ [21–23]. Hence, the Keizer-Levine model was modified to reflect exposure of the RyR to the higher levels of Ca^{2+} present in subspace during Ca^{2+} release.

Thus far, descriptions of the electrical membrane events and Ca^{2+} dynamics have been presented. To complete modeling of whole cell EC coupling, the addition of force generation by the myofilaments is necessary. The Rice-Jafri-Winslow model improves upon the JRW model [24] by incorporation of an isometric force generation model [25]. The force generation model includes

three cooperative mechanisms 1) cross-bridge binding increases the affinity of troponin for Ca^{2+} ; 2) binding of a cross bridge increases the rate of formation of neighboring cross bridges and that multiple cross bridges can maintain activation of the thin filament in the absence of Ca^{2+} ; and 3) a cooperative mechanism designed to simulate end-to-end interactions between adjacent troponin and tropomyosin. The model simulates the steep force-calcium relations and the length dependence seen in experimental studies.

The JRW model and improvements simulates experimentally observed action potential (Figure 2A), Ca^{2+} transients in the bulk myoplasm (Figure 2B) and the dyadic subspace (Figure 2C), and isometric force transients (Figure 2C) consistent with experimental observations. However, using the detailed modeling of channel biophysical properties yielded the ability to simulate experimental interval-force relations, such as restitution and potentiation and force-frequency curves (Figure 3) with much more fidelity than previous models. The force-interval relations are the experimental observation that as the pacing frequency changes, so does the force generated.

The force-frequency curve for guinea pig has been shown to be dome-shaped in experiments with a peak between 2 Hz (in senile guinea pig) and 4 Hz (in young guinea pig) [26]. This has been successfully simulated and predictions about the mechanism are possible (Figure 3). The dome shaped peak normalized

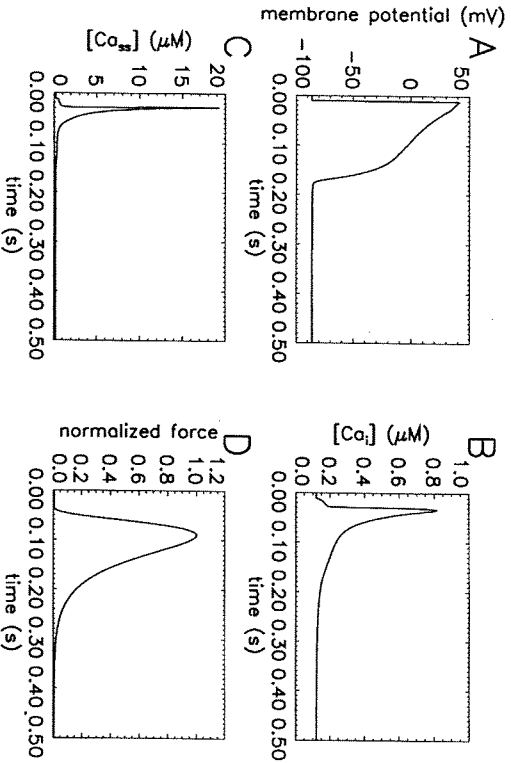


Figure 2. Simulation of an action potential made by the JRW guinea pig ventricular cell model. A. membrane potential. B. bulk myoplasmic Ca^{2+} concentration. C. dyadic subspace Ca^{2+} concentration. D. normalized isometric force.

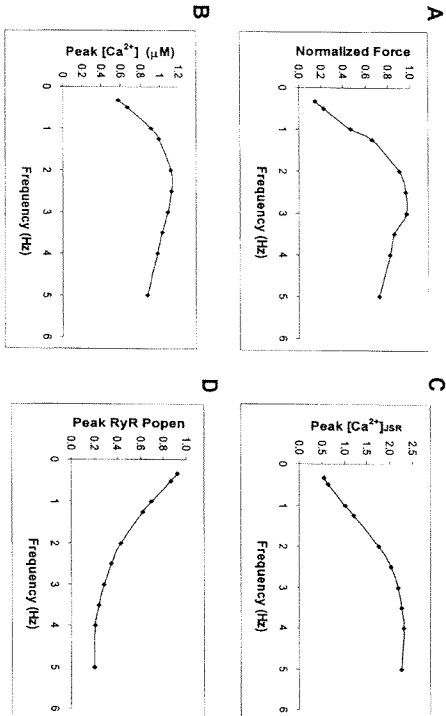


Figure 3. Simulation of the force-frequency relation. A. Peak normalized isometric force B. bulk myoplasmic Ca^{2+} concentration. C. Peak subspace Ca^{2+} concentration D. RyR open probability.

isometric force curve (Figure 3A) is accompanied by a dome shaped peak myoplasmic $[Ca^{2+}]$ curve (Figure 3B). Note that the curve is slightly shifted indicating the force does not depend directly on the peak calcium but takes into account the time course and duration. In the model, as the pacing frequency rises, the SR Ca^{2+} load increases (Figure 3C), consistent with experiment. The model predicts that as the frequency rises, the fraction of channels in the adapted state increases leading to a reduced peak open probability for the RyR (Figure 3D). Because the resting subspace calcium is low ($[Ca^{2+}]_{ss}$), the peak calcium released is the product of the SR $[Ca^{2+}]$ ($[Ca^{2+}]_{SR}$ and the RyR open probability at the time of release. This is demonstrated by the RyR Ca^{2+} flux equation

$$J_{RyR} = \bar{J}_{RyR} P_{open} ([Ca^{2+}]_{SR} - [Ca^{2+}]_{ss})$$

where \bar{J}_{RyR} is the peak RyR Ca^{2+} flux. This suggests that in other species, such as rat, where the force-frequency curve is declining, or during heart failure, where the force-frequency relation is altered, this is most likely due to a different rate of SR loading by SERCA. Recently, SERCA has been shown to alter the force-frequency relation in heart supporting the predictions of the model [27, 28].

In studying mechanical restitution and postextrasystolic potentiation, Rice and co-workers [15] predicted that mechanical restitution was direct result of the

recovery of RyRs from the adapted state and post-extrasystolic potentiation was the result of increased SR loading due to less Ca^{2+} release which leads to increased Ca^{2+} entry due to decreased Ca^{2+} -dependent inactivation during the extrasystolic beat.

Another novel suggestion of the model was the importance of the L-type Ca^{2+} channel in the shortening in action potential during increased pacing rate. Previously, this was primarily ascribed to an increase in the potassium currents. However, the model showed that the L-type Ca^{2+} channel incompletely recovered from inactivation during rapid pacing, leading to reduced current. The importance of the L-type current in determining action potential shape and duration was later confirmed by the experimental work of Linz and co-workers [4, 29].

The mechanism of the termination of Ca^{2+} release is still an open question in the study of EC coupling. Many mechanisms, such as stochastic attrition, adaptation, restitution and local depletion have all been accounted for Ca^{2+} release termination at some time. Stochastic attrition is the random decay of active clusters due to random closure of channels [30]. However, further calculations suggest that this process is unlikely because the probability of simultaneous channel closing is small and local Ca^{2+} does not decrease rapidly to increase this probability [31]. RyR adaptation or inactivation is the possibility of RyR channels inactivating during a release event. However, this process is too slow to account for termination of release [32]. Furthermore, experimental result suggests that RyR inactivation in lipid bilayers is not strong enough to terminate release. Lastly, SR depletion, which occurs during Ca^{2+} release, may affect termination either by RyR open probability dependence on SR load or lack of driving force for Ca^{2+} to release. Recently a lot of attention is being given to proteins present in SR and myoplasm like calsequestrin, triadin, junctin, and calmodulin as data supports their role in RyR channel inactivation, hence in termination. The JRW model, with realistic adaptation of the RyR (a slow incomplete inactivation), suggests that partial depletion of the SR results in termination of Ca^{2+} release. It demonstrates that if SR load is decreased, the flux of Ca^{2+} out of the RyRs is insufficient to maintain CICR.

The JRW model was adapted to describe the canine ventricular cell by Winslow-Rice-Jafri [4] and was also used to study the mechanisms of heart failure in the pacing induced model of heart failure (Figure 4). A normal canine action potential and bulk myoplasmic Ca^{2+} transient are shown in Figures 4 A and B, respectively (solid trace). One defining characteristic of heart failure is a prolonged action potential, the model can be used to assess the impact of the altered functional from changes in gene expression that occur during heart failure. The magnitude of I_{Kr} is reduced by 50% [33], the SERCA pump Ca^{2+} uptake rate is down-regulated 50% [34], and NaCa exchange is up-regulated 100% [35]. Prior to this work the accepted hypothesis was that the changes in

the reduction in the hyperpolarizing potassium currents were the primary cause of action potential prolongation. The model demonstrates that while the changes to the potassium currents only lead to action potential prolongation (Figure 4A; dashed line) as previously thought, the changes to Ca^{2+} dynamics are also significant contributors to action potential prolongation (Figure 4A; dotted line). Furthermore, the model demonstrated that in order to see a typical failing Ca^{2+} transient [36], that has reduced magnitude and prolonged duration, the changes to calcium dynamics are necessary (Figure 4B; dotted line). If only the changes to the potassium currents is included, the calcium transient is actually larger in magnitude (Figure 4B; dashed line).

One of the shortcomings of the JRW model and enhancements is that it is unable to produce graded release. Graded release refers to the proportional

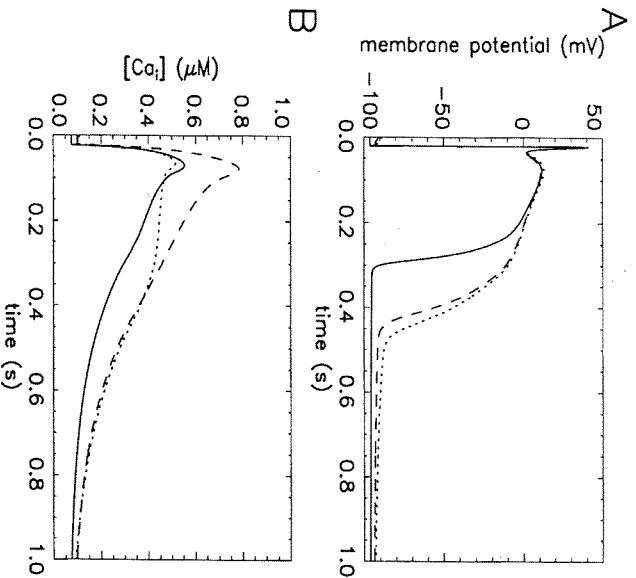


Figure 4. Simulations using the Winslow-Rice-Jafri canine ventricular cell model to study the mechanisms of heart failure. A. Membrane potential during an action potential for the normal (solid), failing with only changes to membrane currents (dashed), and failing with both changes to membrane currents and Ca^{2+} dynamics (dotted). B. Bulk myoplasmic Ca^{2+} concentration for normal (solid) failing with only changes to membrane currents (dashed), and failing with both changes to membrane currents and Ca^{2+} dynamics (dotted).

release of the SR to whole cell L-type channel influx [37]. Since it was a “common pool” model, i.e. all the L-type Ca^{2+} channels and RyRs interacted in one pool, it displays all or none behavior. More explicitly, once the RyRs are triggered, they all open to their fullest extent. This all-or-none behavior is shown in Figure 5A by the almost vertical transitions seen in the Total RyR Calcium flux (solid line). Notice that the L-type Ca flux is at the same level on either side when the transition occurs. The idea that common pool models are incapable of graded release was first postulated by Stern [30]. He suggested that “local control” was needed, i.e. each L-type Ca^{2+} channels only interacted with the nearby RyRs. Hence, the different numbers of L-type Ca^{2+} channels that would be recruited to produce different magnitude Ca^{2+} currents would activate only the local RyRs, resulting in graded release. He demonstrated this in a simplified model.

Rice-Jaffri-Winslow developed a stochastic model of the functional unit which includes the interaction of one L-type Ca^{2+} channel and the 8 nearby RyRs in a diadic cleft [24] (Figure 5B). The channels and parameters are based on the descriptions in the cardiac ventricular myocyte model. The Ca^{2+} profile in a single functional unit is shown in Figure 5C. The stochastic model demonstrated that a biophysically accurate model can produce graded release as expected (Figure 5D), however, each functional unit behaves in an all or none fashion (Figure 5C), i.e. if the functional unit is activated it activated to the fullest extent. The model also demonstrates that even in a stochastic model with a small number of RyRs, termination of release is a result of depletion of the SR. Stochastic attrition and inactivation play little role in the termination of release.

Experiments have shown that EC coupling is defective during heart failure. The stochastic model was used to explore some of the hypotheses behind these defects, such as an increase in the volume of dyadic cleft, alterations in SR load, and changes in the L-type Ca^{2+} current. These parameter studies with the model were unable to sufficiently explain the experimental observation. For this, a more detailed model of the basic mechanism of EC coupling was needed. To this end, Sobie and co-workers developed a model of the Ca^{2+} spark [38]

The new spark model seeks to incorporate the most recent biophysical data to provide a plausible mechanism for EC coupling and the termination of release (Figure 6A). Each release site consists of a single L-type Ca^{2+} channel in the T-tubule and an array of 50 RyRs in the junctional SR membrane that communicate in the dyadic cleft (Figure 6B). The network SR contains the SERCA pumps that refill the SR. The model also includes the two recent biophysical findings that the observations that RyRs displayed the phenomenon of coupled gating and that their open probability was modulated by SR luminal $[\text{Ca}^{2+}]$.

The phenomenon of coupled gating was observed by Marks and co-workers [39, 40]. In coupled gating, up to four RyRs in blayers were observed to open

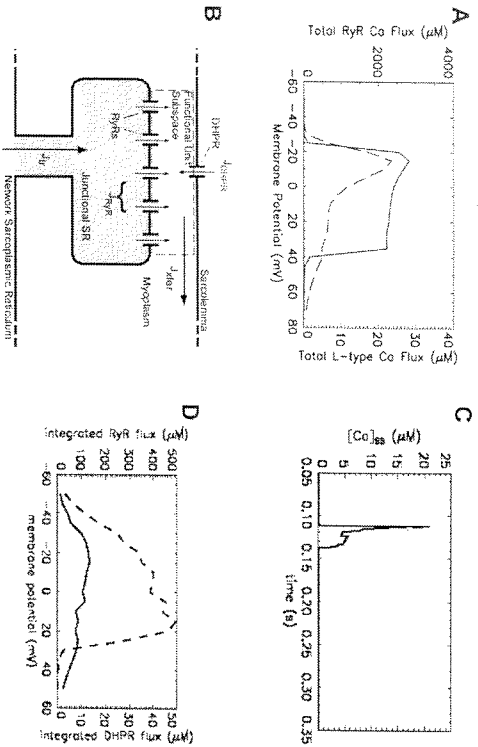


Figure 5. Simulation of local control and graded release. A. The JRV ventricular cell model displays an all-or-none response. Total integrated RyR flux (solid) and total integrated L-type Ca^{2+} current flux (dashed). B. Schematic diagram of the functional unit. C. The dyadic subspace Ca^{2+} concentration displays an all-or-none behavior in the stochastic functional unit model. D. Graded release produced by the stochastic functional unit model with the total integrated RyR flux (solid) and total integrated L-type Ca^{2+} current flux.

and close together as one coupled unit. This coupling is disrupted by the application of rapamycin and FK506, suggesting that FK506 binding protein (FKBP 12.6) was involved in the coupling mechanism. It is believed that the FKBP is arranged regularly in the array of RyRs (Figure 6B) at the site where four RyRs come into close proximity. The FKBP contacts the four RyRs and couples their gating behavior [38].

Experiments by Gyorke and co-workers gives compelling evidence that increases in $\text{SR} [\text{Ca}^{2+}]$ increases the RyR open probability. They show that in a bilayer containing the RyR, setting the membrane so that Ca^{2+} movement would be from the cytosolic side to the luminal side upon channel opening. In this situation, increasing luminal $[\text{Ca}^{2+}]$ increases the channel open probability. [20] Calsequestrin, a Ca^{2+} binding protein found in the junctional regions of the SR, is thought to regulate luminal dependence of the RyR channel in accordance with junction and triadin [41, 42]. Calsequestrin senses luminal Ca^{2+} levels and transmits this information to the RyR channel via intermediate proteins junction and triadin. During Ca^{2+} release when $\text{SR} [\text{Ca}^{2+}]$ declines, free calsequestrin levels increase, which results in inhibition of RyR channels. Similarly at

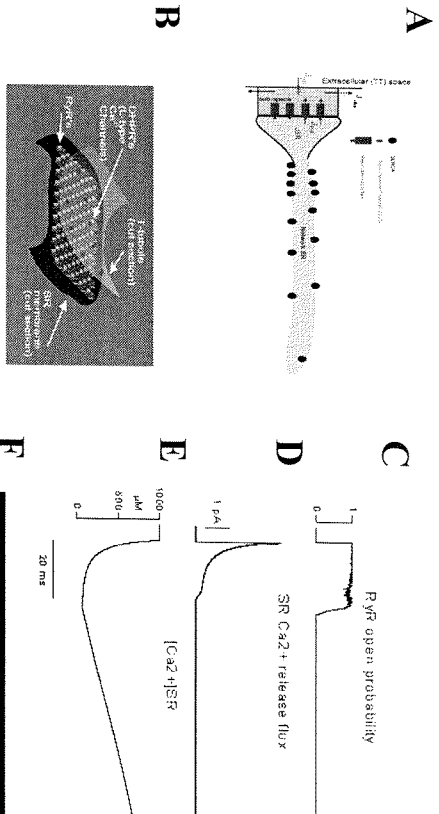


Figure 6. Stochastic model of the Ca^{2+} spark. A. Schematic diagram of the spark model. B. The RyR are packed in an array in the junctional SR membrane and the L-type Ca^{2+} channels spread in the T-tubular membrane in the dyad. C. Simulated RyR open probability during a spark. D. Simulated SR Ca^{2+} release flux via the RyRs during a spark. E. Simulated line scan image of bulk myoplasmic Ca^{2+} during a spark.

elevated SR $[\text{Ca}]$, free calsequestrin levels decrease, hence there are less calsequestrin inhibited RyR channels and increased Ca^{2+} leak. Snyder et al. [43] developed a model of the cardiac ventricular myocyte that included calsequestrin-dependent RyR channel modulation.

The spark model by Sobie and co-workers [38] develops a new model for the RyR by integrating a scheme for coupled gating and for luminal dependence with a simplified gating scheme based on the kinetics of the RyR model proposed by Smith and co-workers [44] (Figure 6A). The model consists of stochastically gated RyRs triggered by a L-type Ca^{2+} channel opening in a restricted subspace. Both subspace $[\text{Ca}^{2+}]$ and junctional SR $[\text{Ca}^{2+}]$ are described by dynamic variables while network SR $[\text{Ca}^{2+}]$ and bulk myoplasmic $[\text{Ca}^{2+}]$ are assumed to remain constant. The RyR open probability stays close to 1 during the spark (Figure 6C). The RyR Ca^{2+} flux peaks upon RyR opening and declines rapidly as the junctional SR $[\text{Ca}^{2+}]$ declines (Figure 6E). As the junction SR $[\text{Ca}^{2+}]$ declines, the open probability of the channel starts to flicker as a result of

the RyR open probability dependence on SR luminal $[Ca^{2+}]$. The reduction in open probability and the coupling between RyR channels eventually results in channel closure. The model produces realistic sparks (Figure 6F) and demonstrates that removal of coupled gating greatly increases spark duration consistent with line scan images from experiments. Furthermore, it suggests that the luminal dependence of open probability plays a crucial role in the termination of release, for when the luminal dependence is removed, sparks fail to terminate reliably. The model also suggests that the depletion of the junctional SR (the SR local to the spark site) reduces RyR open probability so that stochastic fluctuations and coupling can cause closing of the channel.

Cardiac energy metabolism

The primary function of the heart is to work as a pump. To accomplish this, the heart consumes energy to operate the contractile proteins, cycle Ca^{2+} , and maintain ionic homeostasis. During exercise, the human heart rate can increase more than three times the resting level and the energy consumption increases accordingly. Remarkably, the energy production metabolism rises so that the energy supply meets the demand. In order to accomplish, the heart has developed a complex regulatory system that responds to changes in pH, Ca^{2+} , NADH, NAD⁺, ADP, ATP, and P_i [45]. During a wide range of changes in the workload, the levels of metabolic intermediates will remain stable [46-49]. Furthermore, it has been shown that energy levels, namely [ATP], [P_i], and [ADP], can stay constant despite a 3 to 4-fold increase in metabolic intermediates [48]. This suggests that factors such as pH, NADH, NAD⁺, and Ca^{2+} are likely to be the more significant regulators of energy metabolism. Computational modeling has shown to be useful in understanding the complex dynamics of energy metabolism. Furthermore, it can be used to help understand the changes in energy metabolism that lead to cardiac dysfunction in conditions such as hypoxia or ischemia.

Under normal conditions, oxidative metabolism can be divided into three main stages: 1) substrate delivery to the citric acid cycle also known as the tricarboxylic acid (TCA) cycle, 2) the TCA cycle itself, and 3) oxidative phosphorylation. During the first stage of oxidative metabolism, carbohydrates, lipids, and some amino acids are converted into acetyl-Coenzyme A (Acetyl-CoA) through the processes of β -oxidation and glycolysis. Fatty acid oxidation contributes up to 90% of the energy substrate in the heart. The remainder is primarily glucose oxidation. During exercise, glucose contributes a larger fraction of the energy substrates [50]. Once fed to the TCA cycle, the second stage, the acetyl group of acetyl-CoA is completely oxidized to CO₂, resulting in the production of reducing equivalents NADH and FADH₂. Next, in the third stage, these reducing equivalents are oxidized by the electron transport chain,